FATIGUE CRACK GROWTH IN AUSTENITIC STAINLESS STEEL STRUCTURES

B. HENRY, J. BERNARD, Ph. GIEB
Commission of the European Communities
Technology Division, EURATOM Joint Research Center, I-21020 Ispra (Varese), Italy

SUMMARY

Fatigue crack propagation is one of the possible failure processes of the coolant containment structures of type LMFBR (vessel and tubing). This phenomenon is being studied from the point of view of both the general material behaviour and the method of prediction, from the latter, of the structure behaviour taking into account the actual geometry and loading parameters.

1. *Studies on the material behaviour by testing specimens*

Fatigue tests on 8 and 25 mm thick compact tensile specimens in X 6 Cr Ni 18/11 and AISI 304 steels respectively have been undertaken at frequencies ranging from 400 to 4000 cpm, and stress intensity factor range from 25 to 150 kg.mm$^{-3/2}$ both at 20 and 540°C.

Relevant features of the results are as follows:

a) *Room temperature tests:* All the plots of log da/dN vs. log ΔK are straight lines of slopes ranging from 3.6 to 4.2, consistent with the Parris's law: $da/dN = C_0(\Delta K)^n$.

No slope increase is found in the field of low ΔK values.

The load ratio $R = K_{min}/K_{max}$ has a significant influence on the growth rate, which is found to be inversely proportional to (1-R), consistent with Foreman's correlation when the material fracture toughness is supposed much greater than the applied ΔK.

The frequency is found to have no influence both in field investigated in the present work (400-4000 cpm) and at lower frequency as for $R \sim 0$ we find the same growth rate as found by Schwenck *et al.* at 4 cpm on a similar material. To change the specimen thickness from 8 to 25 mm is found to produce a slight increase of the growth rate (factor about 1.3).

b) *Tests at 540°C:* The influence of R on the crack growth rate has the same trend than at 20°C but significantly less pronounced. At low $R(\simeq 0)$, the growth rate is about 2.5 times higher than at 20°C. The frequency has no significant influence in the investigated field (400-1800 cpm) but, on the basis of the comparison with Schwenck *et al.* results at 4 cpm, is thought to be a predominant parameter at lower values.

These results will be discussed in terms of fatigue-creep combined effects on the crack growth rate.

2. *Structural behaviour*

The results presently available concern longitudinally through cracked X 6 Cr Ni 18/11 tubing, 334 mm $\phi_i - 10$ mm thick, at 20°C, pressure cycled at 400 cpm in such a way that the stress intensity factor range, as calculated by:

$$\Delta K = \Delta\sigma_{hoop} \cdot \sqrt{\Gamma r a} \, . M$$

where a is the half crack length and M is the Folias' magnification factor for bulging effects, varied in the field 70-140 kg.mm$^{-3/2}$.

A numerical analysis of a vs. N using Lagrange's polynomial was necessary to reflect the small irregularities in the crack growth rate actually observed. Differentiation gave da/dN and the best fitting parameter C and n of the Parris' correlation were determined using a least mean square fit. The most significant feature of the results is a n value much lower than for the compact specimens and a R-influence not consistent with the specimen behaviour. This result is discussed in terms of the validity of the Folias' factor M used in the ΔK formulation.

1. Introduction

Fatigue crack growth is one of the possible failure modes of the primary containment of LMFBR, for which austenitic stainless steels of the types AISI 304 and 316 are candidate materials.

Fatigue loading originates from various sources such as:

- pressure variations in the coolant loop,
- temperature variations of the liquid metal coolant inducing thermal stresses variations,
- flow induced vibrations producing high cycle fatigue near the fixed points of the structures.

The two latter phenomena are considered of special importance for engineering conditions specific to LMBFR and precisely the high heat exchange coefficient between coolant and structure walls on one side, and the high mass flow in respect to the structure inertia on the other side.

While fatigue phenomena in austenitic stainless steel has been the subject of numerous studies, very few of them have followed the so-called "fracture mechanics approach" or "crack growth approach". This latter one which correlates the crack growth rate to loading and material parameters is thought to be potentially more reliable for the prediction of structural behaviour than the classical one where only a global relation between fatigue stress and failure life is involved, without a special consideration to cracks. As a matter of fact, the high safety coefficient foreseen in the construction codes in respect to fatigue failure data may be regarded as an illustration of the uncertainty of the approach.

Herein are reported the first results of a program aiming at:

a) the study of the influence of different parameters such as temperature, mean load, frequency and sodium environment on the crack growth rate; these studies are done on notched flat specimens,
b) determining whether the behaviour of typical structures such as cylinders, tees, elbows and nozzles loaded in different ways (internal pressure, bending, twisting) may be predicted from specimen data using appropriate formulation for the stress intensity factor or every other loading parameter found to be crack growth rate controlling.

2. Experimental Details

2.1 Specimen Testing

Most of the tests have concerned flat compact tensile specimens (Fig. 1) meeting the ASTM E 399-70T standard except for a reduction in thickness (8 mm) in respect to the other dimensions. These specimens referred to as CT-08 in the following were cut in 10 mm thick plates in X6CrNi 18/11 (DIN) stainless steel (see the measured tensile properties in appendix), the crack being in the rolling direction. No further treatment was done on the

specimen material which was specified to be in the solution annealed and quenched condition. These specimens were sinusoidally loaded on a 6T Instron model 1211 cycler at given load and frequency, the latter ranging between 400 cpm and 1800 cpm. For initiation of the fatigue crack, the mean load and the load range were fixed at 600 kg, corresponding to an initial ΔK value of 60 kg.mm$^{-3/2}$ about (initial notch length at the chevron root = 14 mm). The pre-cracking conditions were progressively shifted to the chosen fatigue conditions within 2 mm of crack extension. In order to check the influence of thickness on the crack growth rate, some other tests have been undertaken on specimens of the same geometry, but with on-scale thickness (25 mm). They are referred to here as CT-25 specimens. They were cut in a 30 mm thick plate in type AISI 304 stainless steel (referred to in the following as EUR-304) in the solution annealed and quenched condition. For these tests, a 5 tons Schenck fatigue machine of the resonance type was used, at a frequency of 4000 cpm approximatively.

In most cases the crack length was measured on one side of the specimens using an optical microscope provided with a measurement reticle. Crack length progresses as small as 0.2 mm could be appreciated by this method. In some other cases, Polaroid pictures of the crack with X20 magnification were taken, still increasing the measurement accuracy to 0.05 mm approximatively.

The same tests were conducted at 540°C as well. The specimens were heated using four 500 W infra-red lamps. Previous calibrations had shown that it was possible to obtain a temperature difference in the crack growth zone smaller than $\pm$ 3°C. The temperature was monitored by a thermocouple sunk in a hole drilled in the specimen mid-plane on the opposite side of the crack, and regulated by an on-off regulation system acting on 10% of the heating power.

2.2 Tube Testing

The specimens were ϕ_e 355 mm - 10 mm thick - 70 cm long tube sections in austenitic stainless steel of the same specification as the 8 mm thick specimens, i.e. X6CrNi 18/11, in the annealed and quenched condition. The tensile properties of the material is reported in appendix and is reasonably similar to those of the plates. A central longitudinal 3 mm wide and 40 mm long slit prolongated by 0.5 mm wide and 5 mm long slits (at each end) was machined in the tube and patched by a rubber membrane glued on the tube and supported by a mild steel 1.5 mm thick sheet sandwiched between the rubber membrane and the tube.

The tube specimen was closed by flanges welded on and connected to the pressure circuit of a Losen-Hansen 60 T fatigue machine (Fig. 2). This last one was operated to a given minimum and maximum pressure, at a frequency of 300 cpm. The pressure was measured by a Bell & Howell pressure transducer connected to a Hottinger 5 kHz bridge and an oscil-

loscope. Maximum measurement errors can be evaluated to 1 kg/cm^2 on maximum and minimum pressure and on pressure range. The constancy of the latter was good, while minimum and maximum pressures fluctuated within 1.5 kg/cm^2.

The crack growth was monitored by X12.8 magnification Polaroid pictures taken with a Zeiss field microscope. The accuracy on the crack length measurement is evaluated to be 0.5%.

3. Results

3.1 Cold Testing on Specimens

Using the plot of the crack length a vs. number of cycles N, the slope $\frac{da}{dN}$ was determined graphically by measurement of the slope of the tangent to the curve in six-eight points for each specimen. On the other side, for the corresponding a value, the stress intensity factor range was determined using:

$$\Delta K = \frac{\Delta P}{B.W^{1/2}} \cdot f(a/w) = \Delta\sigma \,.\, W^{1/2} f(a/w)$$

where: ΔP (kg) = cycling load range; W, B (mm) = specimen width and thickness; f(a/w) = shape function as given in ASTM E 399-70T; $\Delta\sigma = \frac{\Delta P}{BW}$ reference stress range.

In Fig. 3 and 4 are plotted the $\frac{da}{dN}$ vs. ΔK values in bi-logarithmic coordinates for 8 mm and 25 mm thick specimens respectively. The straight lines are graphical fits to experimental points for both specimens tested at the same load rates $R = \frac{\sigma_{min}}{\sigma_{max}}$ at Fig. 3, while on Fig. 4 they are least square fits relative to each specimen. These straight lines express the Paris' type relation between $\frac{da}{dN}$ and ΔK: $\frac{da}{dN} = C_o(\Delta K)^n$. The values of C_o and n as calculated by the least square method for each specimen are summarized in Table I.

The prominent feature of Fig. 3 and 4 is the coherent indication of the influence of the load ratio $R = \frac{P_{min}}{P_{max}} = \frac{K_{min}}{K_{max}}$ on the crack growth rate, which at equal ΔK vary in the same direction. The plots indicate an influence on the constant C_o rather than on the slope. This influence is not evidenced however, by the calculated C_o-values of Table I because those are not associated with a standardized value of n. Quantitatively these results - especially those of Fig. 3 - suggested a variation of $\frac{da}{dN}$ inversely proportional to (1-R), i.e.:

$$\frac{da}{dN} = C \cdot \frac{(\Delta K)^n}{1-R} \qquad \text{eq. (1)}$$

Fig. 5 is a check of the validity of this formulation for the 8 mm thick specimens: while plotting $(1-R)\frac{da}{dN}$ vs. ΔK in bi-logarithmic coordinates, all the experimental points fall in a narrow straight band with a scattering which is not more correlated with R-values. This formulation appears as a simplification of Foreman's relation[1]:

$$\frac{da}{dN} = \frac{C(\Delta K)^m}{(1-R)K_c - \Delta K} \qquad \text{eq. (2)}$$

which could be adopted in situations where ΔK is much smaller than $(1-R)K_c$ in the whole testing range. This condition is fairly fulfilled in our own case: admitting for K_c a typical value of 600 kg.mm$^{-3/2}$ as derived from burst tests of tubing of the same material[2] and for R = 0, our maximum value of ΔK (~130 kg.mm$^{-3/2}$) is 5 times smaller than $(1-R)K_c$. In the opposite case, where R has its maximum value, the investigated range of ΔK is probably too small to let appear its influence in the denominator of eq. (2).

In Fig. 5 have been incorporated the results of one specimen (CT-08-EUR-304-1) cut in the same plate as the 25 mm thick specimens. These results do not differentiate from the other ones, showing that eventual differences in the behaviour of 8 mm thick and 25 mm thick specimens are not produced by differences in material quality.

The reduction of the results relative to 25 mm thick specimens by the parameter $(1-R)\frac{da}{dN}$ (Fig. 6) seems as well valid in spite of a greater scattering. Fig. 4 and 6 incorporate results of two 25 mm thick specimens tested at 1800 cpm, i.e. the frequency involved in the tests of the 8 mm thick specimens; a small frequency effect may be deduced from these results, which remain however comparable to the scattering band.

It is of interest to note at this point that our results for R = 0 and 8 mm thick specimens fit exactly previous results by James and Schwenck obtained at R ≃ 0 and frequency ranging in 2-400 cpm[3], as shown in Fig. 3. One can therefore deduce that frequency is practically without influence on crack growth rate at room temperature in stainless steel in a range as large as 2-4000 cpm.

As a consequence it is possible to compare the results of 8 mm and 25 mm thick specimens attributing the difference in behaviour essentially to the thickness.

The plots in Fig. 3 show actually a greater growth rate at equal ΔK for the thicker specimens, with however an overlapping of the scattering bands in the high ΔK field. This thickness effect is supported by the dimension of the plastic zone size, evaluated by $r_p = 1/2\pi.(\Delta K)^2/(2\sigma_Y)^2$ as suggested by Johnson and Parris[4]. The result is 1.7 mm approximatively for our maximum value of ΔK (130 kg.mm$^{-3/2}$), which is small but not neglectible relatively to the 8 mm specimen thickness.

3.2 Testing at 540°C on Specimens

The results are summarized at Fig. 7 and 8. On Fig. 7, each line is the least square fit relative to each specimen. The tendency of the growth rate to increase with R is still evident here and this fact coupled with the clear-cut room temperature behaviour justifies the reduction by the $(1-R)\frac{da}{dN}$ parameter (Fig. 8). The scattering of the experimental points may be due to greater difficulties to measure crack length in the high temperature condition. As a matter of fact, very thin shear lips develop on the edge of the fracture surface in high

temperature fatigue. These lips break suddenly at an unregular rate: the crack length readings are felt to be scattered for this reason.

The influence of frequency in the field 400 cpm - 1800 cpm seems neglectible if one compares (Fig. 8) the results of 2 specimens tested at 400 cpm with all the other ones tested at 1800 cpm. However, the comparison shown at Fig. 7 and 8 with the results of James and Schwenck[3] obtained at the same temperature ($\sim 540^{\circ}C$) but at 4 cpm shows that at such a low frequency the crack growth rate is significantly increased. Any material effect may be excluded on the basis of the previously described similar behaviour of both materials at room temperature. A creep interference in the fatigue process due to the low strain rate is suggested to be at the origin of this behaviour.

Another noticeable feature is the behaviour at low ΔK and high R represented by specimen CT-08-24. While the shape of the $\frac{da}{dN}$ - ΔK plot such as drawn on Fig. 7 is only indicatory, the results could indicate a higher growth rate for very low ΔK values (i.e. < 40 kg. $mm^{-3/2}$) than expected. This result is apparently in contradiction with James and Schwenck findings[3] which support a slope transition exactly in the opposite direction. However, James & Schwenck results concerned fatigue at load ratio practically 0 instead of a high value (0.74) in our case. One may therefore suspect in this behaviour another interference of creep crack growth due to the high level of the load static component. This phenomenon would be evidenced especially in the low ΔK field due to low pure fatigue growth in these conditions. Supplementary testing is in any case necessary for a more precise description of material behaviour in this field of high R and low ΔK values as well as for low frequency behaviour, in order to understand better creep-fatigue interferences in the crack growth process.

The room temperature and $540^{\circ}C$ crack growth rate are compared in Fig. 6 in terms of $(1-R)\frac{da}{dN}$. The difference although significant remains small at the frequency involved (1800 cpm).

3.3 Tests on Tubes

Two tubing specimens were tested in practically similar conditions, excepted for the tube thickness along the crack path which was 9.8 mm for the first specimen and 8.7 mm for the second one. The program of the tests for both tubes was as follows:

- crack initiation and 1st phase: pressure cycling between $p_{min} = 8$ atm and $p_{max} = 42$ atm. These conditions represented a nominal stress range $\Delta\sigma$ of 5.80 kg/mm^2 for the first tube and of 6.53 kg/mm^2 of the somewhat thinner second tube.
- 2nd phase: pressure cycling between $p_{min} = 15$ atm and $p_{max} = 30$ atm. This corresponded to a nominal stress range of 2.56 kg/mm^2 for the first tube and 2.88 kg/mm^2 for the second tube.

The optical measurements of the crack length were taken as regularly as possible (i. e. at intervals of 5.10^4 cycles), after the cracks had initiated along 2. 5 mm on each side of the original notch. No particular attention has been given to the rather different crack growth rate on both sides (the values of which were actually averaged), which is felt to be the consequence of continuous random variations of geometrical and metallurgical characteristics of the tubes along the growing crack. A graphical presentation of the average half crack length as a function of the number of cycles results in a reasonably smooth curve that presents some peculiarities in both cases. Indeed, for the first tubes the tests were run on the basis of approximatively 5 to 8 hours uninterrupted cycling. It has been noticed that the a/N graph sometimes shows a distinct step after an interruption. As no consistency in the sign of these steps has been found, no conclusions, as far as this phenomenon is concerned, have been inferred. On the other hand, since the progression of the crack measured day-by-day was sufficiently regular, a Lagrange type interpolation formula has been considered as a most appropriate numerical analysis method in this case, since it reflects also the small discontinuous variations in the slopes of the a/N curve taken punctually. In the second test, the major part of the cycling was done without interruption as this was considered to be a good approach towards the better understanding of the fatigue crack growth problem. Differentiation of the Lagrange polynomial allowed to calculate punctually the crack growth rate. For every crack length and corresponding phase of cycling, the stress-intensity factor range ΔK was calculated as follows:

$$\Delta K = \Delta\sigma(\pi . a)^{1/2} . M$$

where: a is the growing 1/2 crack length; M is a magnification factor for the curvature effect.

As far as M is concerned, the calculations of ΔK were based on the Folias calculations [5] where M is given as a function of λ and $\lambda = a/\sqrt{Rt\,[12(1-\nu^2)]^{1/4}}$; R and t respectively average radius and thickness of the tube. The results of these calculations in both cases were plotted in a log. log diagram (Fig. 9). In this diagram a calculated line of a CT specimen (CT-08-14; see Table I) is represented. Noticeable divergences appear between the results of the two tubes and a great discordance appears between these results and those of the CT specimen. Considering this, some doubts have arisen about the validity for this type of tests of the M value as determined by the Folias curve. Indeed, from Fig. 9 it appears clearly that for a given $\frac{da}{dN}$ the value of ΔK is consistently too high. When the best-fitting straight lines are recalculated on the basis of a shape factor M = 1, these lines are shifted as can be seen in Fig. 9. Two comments can be made here: there is a better agreement of the results of the two tubes between themselves and both results are in better agreement with the CT results; secondly, the lines corresponding to the lower R value of 0. 19 (1st phase of the cycling) is closer to the CT specimen's line, for which R = 0, than the lines corresponding to the R value of 0. 5 (2nd phase). This is the correct way it should be. An effort was made

to define a better M vs. λ law. Considering the CT specimen results as a reference, all M values were recalculated so that in every point, for a given $\frac{da}{dN}$ and λ , the ΔK would fit the CT specimen data. In both cases, about 20 experimental points were considered, the value of $\frac{da}{dN}$ being consistently corrected by a factor (1-R). The new values of M that were found, are plotted in Fig. 10. A least-square fitted line has been calculated passing through the origin: $M = 1$ for $\lambda = 0$. The resulting law is: $M = 1 + 0.095\lambda$. All experimental results were recalculated using this formula and the C and n parameters (Parris law) were computed. The resulting lines are as shown in Fig. 11. The coincidence with the CT specimen data becomes fairly satisfactory. One may note at this point that other authors[6] on the basis of burst testing results already proposed M values significantly lower than those calculated by Folias.

4. Conclusions

The reported tests on compact tensile specimens while confirming previous published data on fatigue crack growth in AISI 304, have extended them as far as effects of load ratio and frequency are concerned. These effects are compatible with Foreman's prediction at room temperature and reflect a possible interference of creep at 540°C, low frequency and/or high load ratio. The study of this effect calls for supplementary testing in view of a quantitative evaluation.

The tests on cylinders showed that the prediction of the structural behaviour on the basis of specimen testing is not so easy even for this simple geometry. One may indeed deplore the lack of reproducibility of the two similar tests but it appears seriously that as soon as the stress intensity factor is accepted as controlling parameter of the fatigue extension rate, its presently available formulation for longitudinally cracked tubing does not give correct results.

A definitive conclusion in this sense as well as the proposal of an alternative correction for curvature in stress intensity factor formulae which would be sufficiently general, entails tests on other diameter and thicknesses, presently in progress.

Acknowledgements

Support received from the joint laboratories of the Technology Division (MM. Dufresne and Jung) and technical assistance from MM. Manzotti and Tognoli are gratefully acknowledged.

The interest shown in this work by Interatom GmbH-Bensberg, Germany, which supplied the plate and tube materials, is highly appreciated.

References

/1/ R. G. FOREMAN et al., Journal of Basic Engineering, Vol. 89 (1967)

/2/ B. HENRY, J. BERNARD, "Fracture criteria in Type AISI 304 SS Tubing", in Annual Report 1972. Euratom JRC, Ispra, Italy, (EUR-report to be published)

/3/ L. A. JAMES and E. B. SCHWENK, Jr., "Fatigue Crack Propagation Behaviour of Type 304 SS at Elevated Temperature", Metallurgical Transactions, Vol. 2, Febr. (1971)

/4/ H. H. JOHNSON and P. C. PARRIS, "Subcritical Flaw Growth", Eng. Fract. Mech., Vol. 1 (1968)

/5/ E. S. FOLIAS, "On the Effect of Initial Curvature on Cracked Flat Sheets", Int. J. of Fract. Mech., Vol. 5, No. 4, Dec. (1969)

/6/ M. B. REYNOLDS, GEAP-5637-June (1968)

TABLE I

Specimen reference	R	C_o	n	notes	
CT-08-21	0.07	$3.065 \cdot 10^{-12}$	3.84	Frequency = 1800 cpm. Instron Cycler	Thickness = 8 mm
" -14	0.09	$1.164 \cdot 10^{-11}$	3.53		
CT-08- 3	0.33	$1.261 \cdot 10^{-12}$	4.11		
" - 4	0.33	$1.642 \cdot 10^{-11}$	3.54		
CT-08- 5	0.55	$3.656 \cdot 10^{-11}$	3.47		
" - 6	0.55	$4.847 \cdot 10^{-11}$	3.38		
CT-08- 1	0.69	$4.657 \cdot 10^{-11}$	3.44		
" - 2	0.69	$3.334 \cdot 10^{-11}$	3.52		
CT-08-20	0.8	$3.807 \cdot 10^{-12}$	4.14		
CT-25- 9	0.066	$2.403 \cdot 10^{-12}$	3.977		Thickness = 25 mm
CT-25- 8	0.167	$5.771 \cdot 10^{-12}$	3.771		
CT-25- 2	0.167	$1.593 \cdot 10^{-11}$	3.497	Frequency = 4000 cpm. Schenck cycler	
CT-25- 1	0.36	$6.615 \cdot 10^{-11}$	3.344		
CT-25- 3	0.375	$1.602 \cdot 10^{-9}$	2.608		
" - 4	0.375				
CT-25- 5	0.60	$2.508 \cdot 10^{-10}$	3.13		

APPENDIX

Tensile Properties of the Plate and Tubing Materials Used in the Experiments

a) X6 CrNi 18/11, 10 mm thick plates (for CT-08 specimens)

ϕ 6 mm cylindrical specimens. Gauge length for deformation: 10 x diam.

	$\sigma_{0,2}$ (kg.mm^{-2})	σ_R (kg.mm^{-2})	A (%)	
Longitudinal	24.1	58.6	61	20°C. Averaged values on 3 spec.
Transverse	21.5	55.4	62.7	
Longitudinal	12.2	38.5	35.9	540°C. Averaged values on 2 spec.
Transverse	13.0	38.9	34.2	

b) Type AISI 304-EUR, 30 mm thick plates (for CT-25 specimens)

ϕ 10 mm cylindrical specimens. Gauge length for A% measurement: 10 x diam.

Longitudinal	22.4	57.6	55.2	20°C. 3 spec.

c) X6 CrNi 18/11, ϕ_e 355 mm - 9.8 mm thick tubing

ϕ 5 mm cylindrical specimens. Gauge length for A% measurements: 8 x diam.

Longitudinal	21.3	58.3	42.9	20°C. 3 spec.
Transverse	20.6	57.6	41.7	
Longitudinal	11.5	40.3	33.6	540°C. 3 spec.
Transverse	12.2	40.1	33.6	

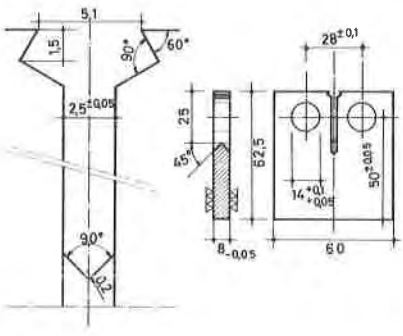

Fig. 1 : C.T. - 08 Specimen

Fig. 2 : View of the experimental arrangement for tubing pressure cycling

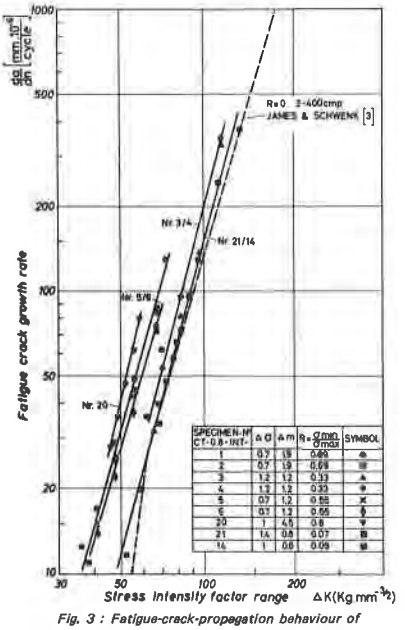

Fig. 3 : Fatigue-crack-propagation behaviour of typ X6 Cr Ni 1811 stainless steel at 20°C
Frequency: 1800 cpm
C.T. specimen, 8 mm thick

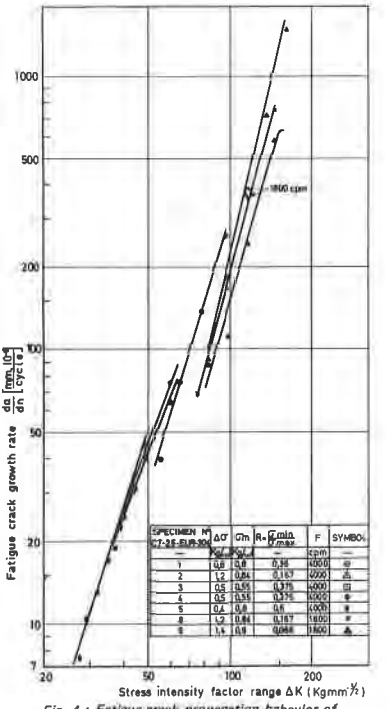

Fig. 4 : Fatigue-crack propagation behavior of type AISI-304 stainless steel at 20°C
C.T. Specimen, 25 mm thick

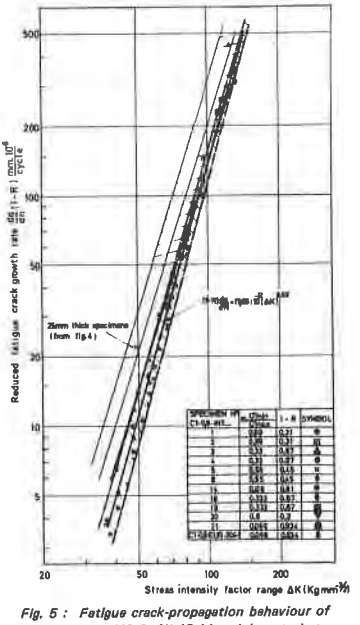

Fig. 5 : Fatigue crack-propagation behaviour of type X6 Cr Ni 18-11 stainless steel at 20°C
Frequency: 1800 cpm
C.T. Specimen, 8 mm thick

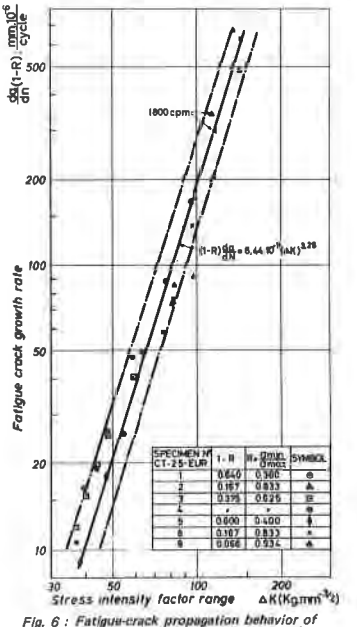

Fig. 6 : Fatigue-crack propagation behavior of type AISI-304 stainless steel at 20°C
C.T. Specimen, 25 mm thick
Frequency : 4000 cpm

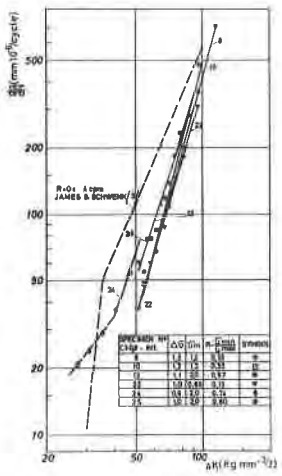

Fig. 7 : Fatigue crack propagation behaviour of type X6CrNi 1811 stainless steel at 540°C
C.T. specimen, 8 mm thick
Frequency: 1800 cpm

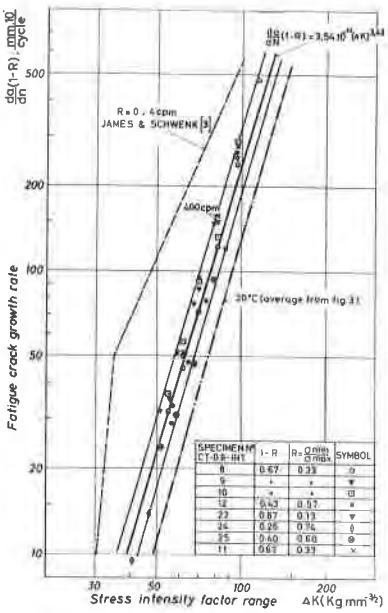

Fig. 8 : Fatigue crack propagation behaviour of type X6CrNi 1811 stainless steel at 540°C
C.T. specimen, 8 mm thick
Frequency: 1800 cpm

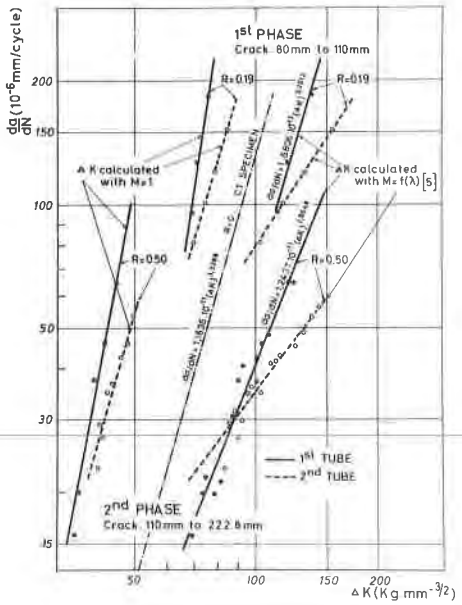

Fig. 9 : Longitudinal fatigue crack grow in ϕ_e 354 mm - 10 mm tubing
crack growth: 50 mm to 222,8 mm

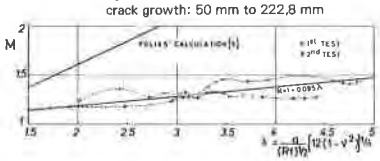

Fig. 10 : Values of the magnification factor M resulting from the fit of crack growth rate to that of C.T. specimens

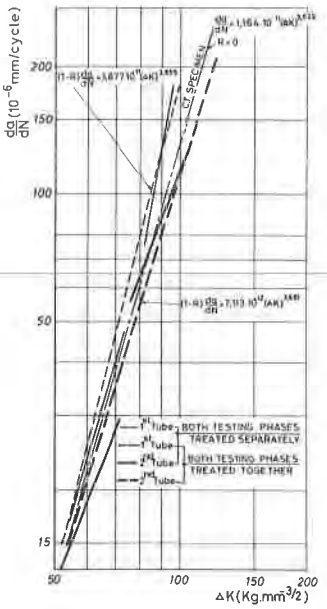

Fig. 11 : Longitudinal fatigue crack growth in ϕ_e 354 mm-10 mm thick tubing